12TH INTERNATIONAL SYMPOSIUM ON FLOW VISUALIZATION
September 10-14, 2006, German Aerospace Center (DLR), Göttingen, Germany

PITCHING AIRFOIL BOUNDARY LAYER INVESTIGATIONS

M. Raffel, H. Richard, K. Richter, J. Bosbach, W. Geißler
Institute of Aerodynamics and Flow Technology of the German Aerospace Center DLR
D-37073 Göttingen, Germany

Keywords: *dynamic stall, pitching airfoil, boundary layer, PIV*

ABSTRACT

The present paper describes an experiment performed in a transonic wind tunnel facility where a new test section has been developed especially for the investigation of the unsteady flow above oscillating airfoils under dynamic stall conditions. Dynamic stall is characterized by the development, movement and shedding of one or more concentrated vortices on the airfoils upper surface. The hysteresis loops of lift-, drag- and pitching moment are highly influenced by these vortices. To understand the very complicated unsteady flow involved, a detailed knowledge of the instantaneous flow fields is of crucial importance. With the application of the described measuring techniques it is expected to gain more insight into the problem. Results from these tests are ready for comparison with numerical data.

1 INTRODUCTION

In recent years the dynamic stall problem on helicopter rotor blades gained considerable interest in both Europe and the US. The dynamic stall problem has been investigated for a long time; a large number of papers and publications exist on this subject (see i.e. [1], [2]). However, the complexity of the flow is high and the problem is still not completely understood. Dynamic stall limits the flight envelope of the helicopter. It is therefore of high interest to influence dynamic stall in such a way that high drag and negative pitching moment peaks are avoided without loosing lift. For the consequent development of reliable dynamic stall control technologies (see [3]) it is inevitable to be able to understand the complex flows involved. The most important features of the dynamic stall process are displayed in Fig.1. Fig.1 shows vorticity contours derived from PIV data measured at about 19° upstroke of a OA312 airfoil under deep dynamic stall conditions. A strong vortex is developing and moving along the airfoil upper surface. Only a short time later this vortex lifts off the surface and is shed into the wake. A counter rotating vortex is developing at the airfoil trailing edge. These events have a strong impact on lift-, drag- and pitching moment: When the vortex leaves the airfoil the drag is increasing and the pitching moment shows a strong negative peak. At the same time the lift which has reached a considerable higher level compared to the steady case breaks down immediately. Strong hysteresis effects occur during the down stroke part of the airfoil motion. It is well known from previous investigations [5], that flow in a very limited area at the leading edge is supersonic although the main flow has a low Mach number of M = 0.3. The supersonic bubbles are terminated by very short but strong shock waves. It is assumed that the compressibility effects serve as a trigger of the dynamic stall process. Due to these observations of dynamic stall vortices with

strong vorticity contents and compressibility effects triggering the dynamic stall process it is very obvious that new suitable measuring techniques are necessary to look into the details of these different flow phenomena. The PIV technique [6] gives the opportunity to measure instantaneous velocity fields from which the vorticity distribution can directly be derived.

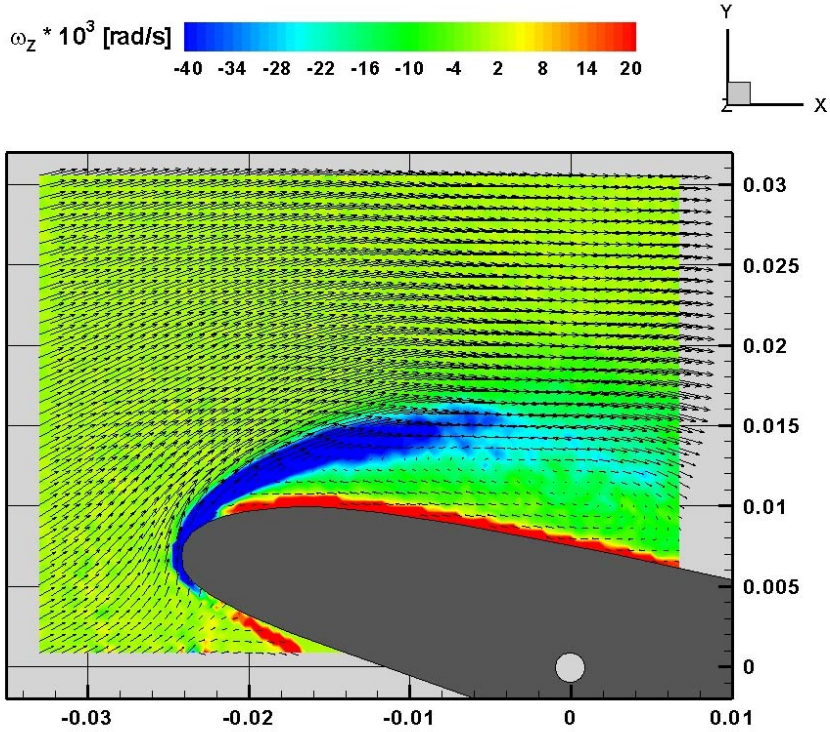

Figure 1: Development of the dynamic stall above a pitching airfoil in upstroke motion

2 FACILITY DESCRIPTION AND TEST MATRIX

A new test section for dynamic stall experiments has been developed within the scope of the German project AROSYS (Active ROtor SYStems). This test section is now equipped with a servo motor to drive the model. The dimensions of the new test section are: Span: 0.1 m, Height: 0.35m. The motion of the model can either be sinusoidal (mean incidence: $\alpha_0 = 10°$, amplitude: $\alpha_1 = \pm 10°$, oscillation frequency: f = 11Hz) or a ramp-type motion, i.e. with a constant angular velocity. The motor rotates a circular plate which is plain with the back wall of the test section. The airfoil model is rigidly attached to this plate; a 4:1 gear is placed between motor and plate. To control the airfoils motion an angular pick-up is mounted directly on the moving plate. Eight pressure tabs, four at each side wall are located directly behind the wind tunnel nozzle to control the Mach number inside the test section. Incidence combinations and frequency selections can be made with the motor control unit. Fig. 2 shows an overview of the test setup. The wind tunnel used during these tests is of blow down type: the tunnel test section is connected to a vacuum chamber via a tube system. The flow is set into motion after opening a remotely controlled valve. The measuring time depends on the Mach number

of the present test and is of the order of 30 - 45 seconds. The model is fixed to a circular plate opposite of the observation window and is suspended in a bearing inside the window glass. The axis of rotation is at quarter chord. The Mach number of the tunnel is selected by a remotely controlled adjustment of a blocking rake which is installed downstream of the test section. The PIV setup consisted of a double oscillator Nd-Yag laser with a pulse energy of 320 mJ. Two spherical and one cylindrical lens are needed to generate the light sheet. A 12 bit camera of 1376x1040 pixels resolution equipped with a 150mm lens or a 600mm zoom lens has been used. During the first phase of the test, the laser is mounted in front of the test section. During this in-flow measurements the laser light sheet illuminated the mid section of the model upper surface through the wind tunnel nozzle. During the later cross-flow tests, the light sheet was adjusted to be parallel to the leading edge (see Fig. 2). The parameters of the PIV processing are summarized in Table 1.

Table 1: Test parameters

Profile (100mm cord length)	OA312	Field of view cross -flow	12.3mm x 9.3mm
Free stream Mach number	0.2	Field of view in-flow	39.5mm x 29.9mm
Mean incidence angle	10°	Interrogation window cross -flow	24px ~ 0.22mm
Incidence angle variation	± 10°	Interrogation window in-flow	24px ~ 0.71mm
Pitching frequency	11Hz	Interrogation step width	12px

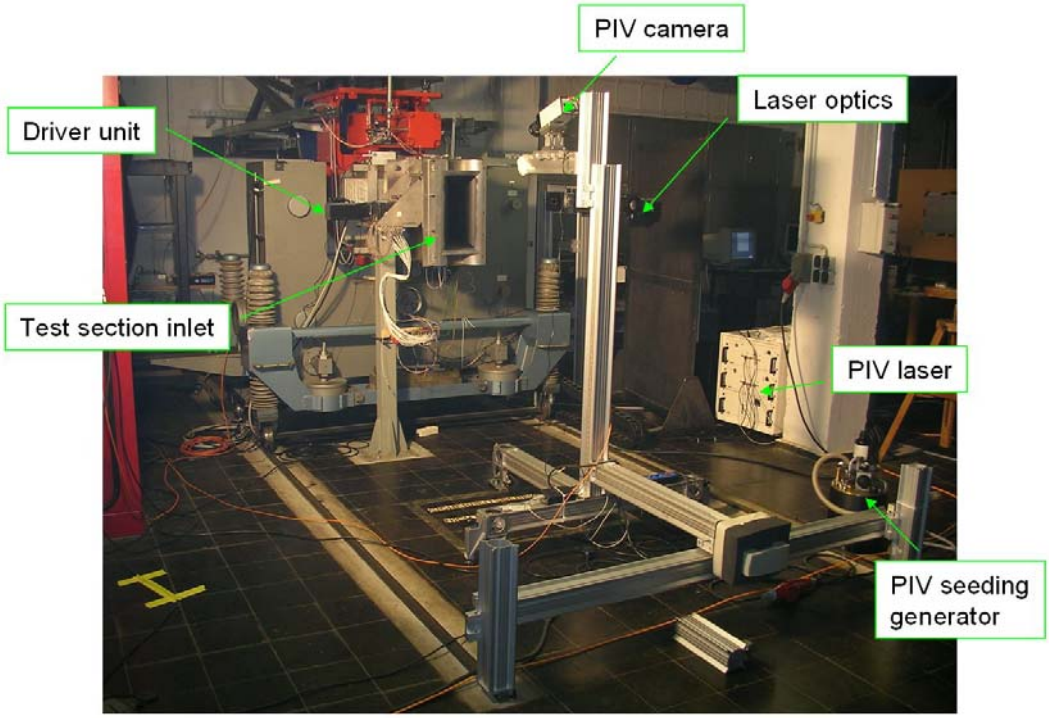

Figure 2: Transonic dynamic stall / pitching airfoil test setup

During the present dynamic stall tests the Mach number was varied between M = 0.2 and M = 0.4. The corresponding measurement times were large enough to measure about 100 images with the PIV system. For the phase locked measurements of the laser system a trigger signal was given from the motor to the laser. Changing the time delay from the trigger signal, the complete period of oscillation could be covered step by step. The servo motor realizes also the selected mean incidence and amplitude of oscillation. This value is stable over a sufficiently long time period. Of importance is also the stability of the trigger signal produced by the motor control unit because this signal is used in order to synchronize the PIV equipment.

3 RESULTS AND DISCUSSION

In the present section some selected experimental data will be presented. The measurements are done in a phase locked manner, i.e. the phase delay from a trigger signal of the servo motor is selected. At each phase about 30 single pictures are taken. 5 upstroke and 5 downstroke phases were measured in order to cover the complete cycle. The phases are concentrated in the region where the important changes due to influences of turbulence eddies have to be expected. Figure 3 shows the orientation of the measurement plane and PIV raw image for the in-flow measurement configuration, which has been performed with a 150mm lens. The contrast, seeding homogeneity and data quality obtained for this observation field size and orientation was relatively good. The boundary layer has not been resolved because of light scattering at the curved leading edge shape and the limits of the optical resolution.

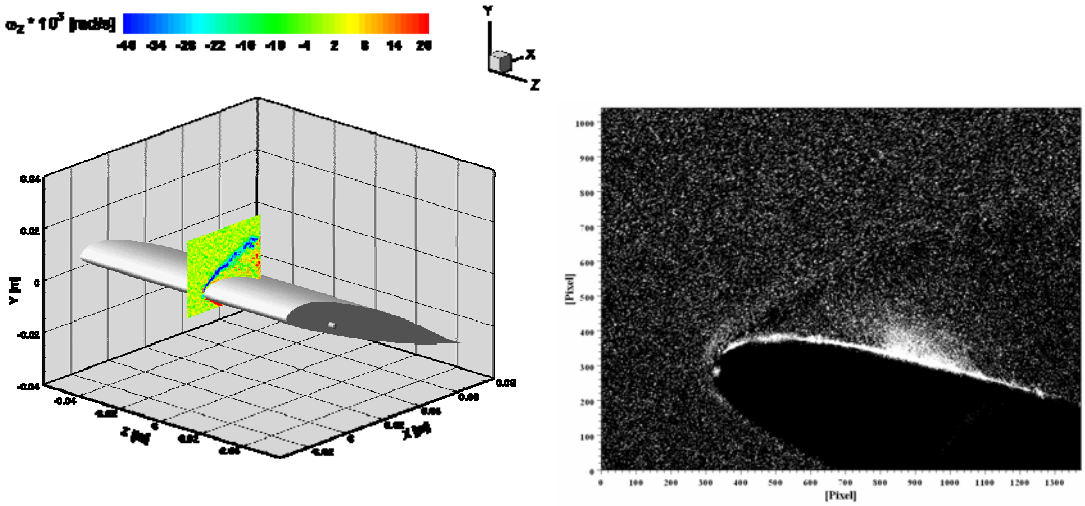

Figure 3: Orientation of the measurement plane and PIV raw image for the in-flow measurement configuration

All the images obtained during the measurement were first pre-processed using a high pass filter, then a binarization filter and finally an anti-alias filter in order to increase the signal to noise ratio. A multi-grid algorithm was applied to process the image, which uses a pyramid approach by

starting off with large interrogation windows on a coarse grid and refining the windows and grid with each pass. A window size of 64 x 64px was used as initial sampling window and 24 x 24px as final window size. The evaluation step width was 12px and the peak fitting routine used the Whittaker reconstruction. The vorticity contours for the early phase of the cycle have been found to be relatively smooth: turbulence and friction are limited to a thin boundary layer (see Fig. 4). Severe separation starts occurring with large recirculation zones at an incidence angle of about 16° upstroke. The vorticity distributions are now lifted from the airfoil surface close to the leading edge upper surface. In Fig. 4, the vorticity contours are color coded from blue (clockwise rotation) to red (counterclockwise rotation). It can be seen that a layer of counter rotating vorticity is located below the clock wise rotating vorticity. This „negative“ vorticity is created at the airfoil trailing edge where reversed flow is developing and moving up stream all the way towards the vicinity of the leading edge.

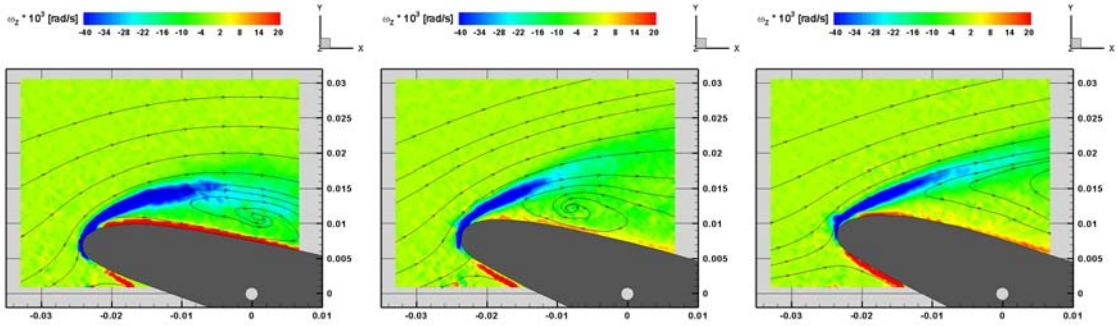

Figure 4: Development of the dynamic stall above a pitching airfoil in **upstroke** motion (averaged PIV results as color coded vorticity and streamlines for 16°, 18°, 20°)

Fig. 5 shows color coded vorticity as measured by PIV and streamlines derived from the same data for downstroke motion. It can be seen that the measured vorticity distributions show similar features than the upstroke results. However, the streamlines differ and do not exhibit the strong recirculation that can be found in the results of the upstroke motion (16° and 18° incidence).

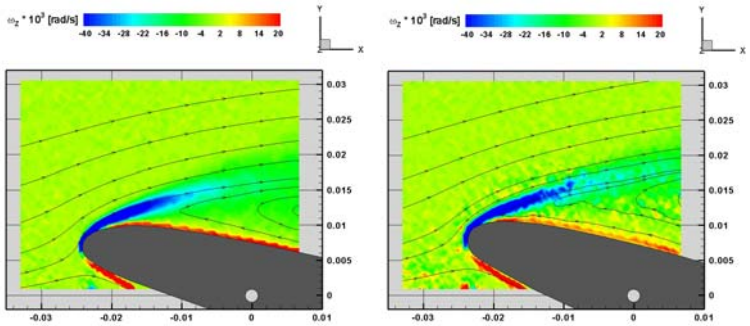

Figure 5: Development of the dynamic stall above a pitching airfoil in **downstroke** motion (averaged PIV results as color coded vorticity and streamlines for 16°, 18°)

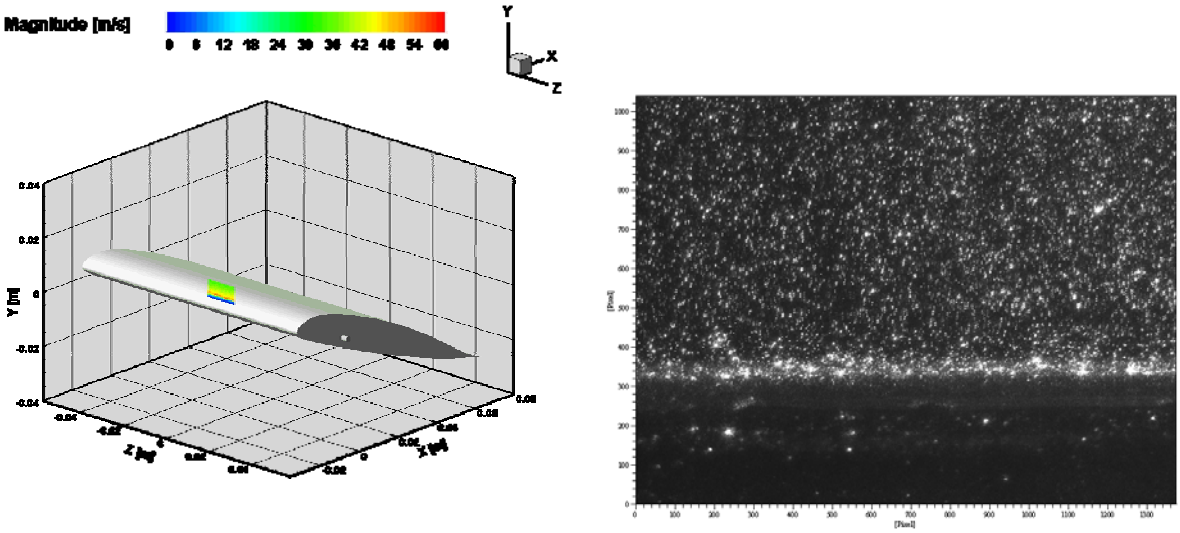

Figure 6: Orientation of the measurement plane and PIV raw image for the cross-flow measurement configuration

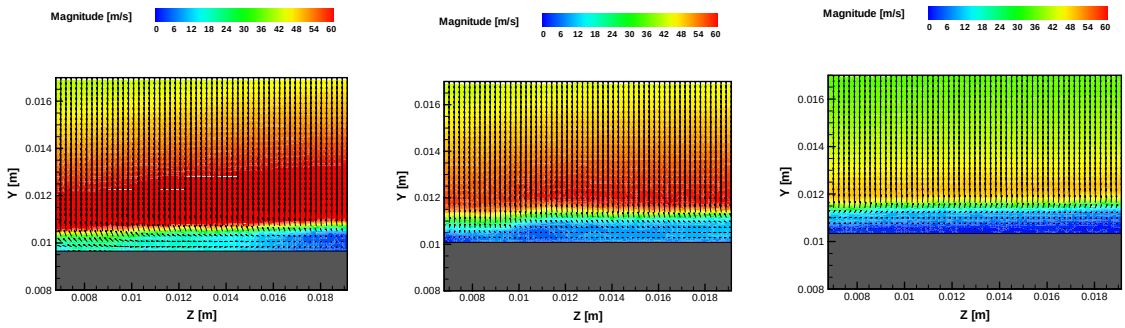

Figure 7: Development of the dynamic stall above a pitching airfoil in **upstroke** motion (averaged PIV results as color coded vorticity and streamlines for 16°, 18°, and 20°)

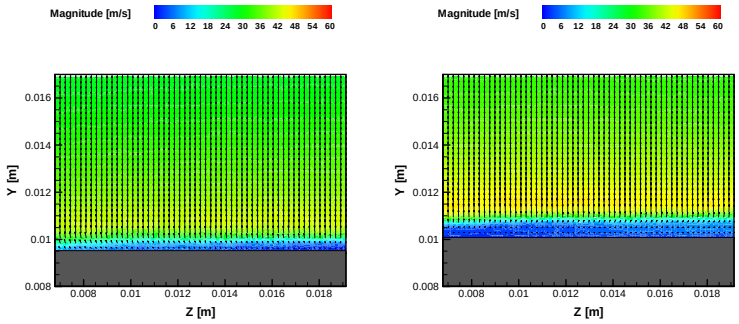

Figure 8: Development of the dynamic stall above a pitching airfoil in **downstroke** motion (averaged PIV results as color coded vorticity and streamlines for 16°, 18°)

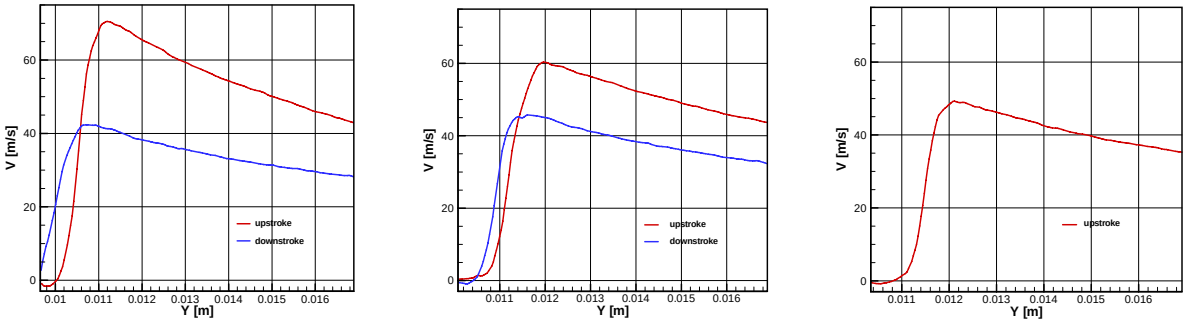

Figure 9: Wall normal velocity profiles for the up- and downstroke motion (16°, 18°, and 20°)

Figure 6 shows the orientation of the measurement plane and PIV raw image for the cross-flow measurement configuration, which has been performed with a 600mm lens. Again, contrast, seeding homogeneity and data quality obtained for this observation field size and orientation were of good quality. The mean particle image diameter is slightly increased with respect to the results found for the in-flow arrangement. The boundary layer has been resolved because of reduced light scattering at the leading edge (linear shape in this direction) and the enhanced optical resolution.
The thin vorticity layer close to the leading edge and the over velocities in the outer areas can clearly be seen Fig. 7 (upstroke) and Fig. 8 (downstroke). Wall normal velocity profiles are shown in Fig. 9. The differences between the up- and the downstroke motion and the separation starting between 18° and 20° upstroke can be seen as well.

4 CONCLUSIONS AND OUTLOOK

The non-intrusive Particle Image Velocimetry (PIV) has been applied in a transonic flow at very high spatial resolution for the investigation of the unsteady boundary layers on pitching airfoils. The dynamic stall problem has been investigated in a new wind tunnel test section equipped with a driving motor to oscillate the model. Here, in a first step the Particle Image Velocimetry has been applied to the clean airfoil. In future investigations the boundary layer manipulation by leading edge vortex generators will be realized and investigated on oscillating models. The experimental data obtained during these tests show the main features of the dynamic stall process at a high spatial resolution: development, growth and shedding of the dynamic stall vortex. These data are in good agreement with corresponding numerical results obtained with a time-accurate 2D-NS-code. It has been found that the development, growth and shedding of the dynamic stall vortex takes place in a very small time window of only a few incidence degrees. To catch the most important events of this process a sufficient number of PIV-sequences had to be taken during this part of the loop. Such data includes the turbulence content of the flow which is not included in the numerical data. It is expected that a more detailed analysis of the highly resolved measurement data allows for an improved tuning of the turbulence model parameters and – for the later tests – a better understanding of flow control devices.

REFERENCES

1. McCroskey, W.J., "The phenomenon of dynamic stall", NASA TM 81264, 1981.
2. Carr, L.W., McCroskey, W.J., "A review of recent advances in computational and experimental analysis of dynamic stall", Proc. IUTAM symposium on Fluid Dynamics of High Angle of Attack, Tokyo, Japan, 1992.
3. Geissler, W., Raffel, M., "Dynamic Stall Controlby Airfoil Deformation", Nineteenth European Rotorcraft Forum, Cernobbio (Como), Italy, Proceedings pp. C2-1 C2-13, Sept. 14-16, 1993
4. Geissler, W., Vollmers, H. “Unsteady Separated Flows on Rotor-Airfoils -Analysis and Visualization of Numerical Data-” 19th European Rotorcraft Forum, Avignon, France. Proceedings pp. 79.1-79.12, Sept. 15-18, 1992
5. Carr, L.W., Chandrasekhara, M.S., "Compressibility Effects on Dynamic Stall", Prog. Aerospace Sci. 32, pp. 523-573, 1996
6. Raffel, M., Willert, C., Kompenhans, J., “Particle Image Velocimetry - A Practical Guide”, Springer, 1998
7. Raffel, M., Favier, D., Berton, E., Rondot, C., Nsimba, N., Geissler, W. “Micro-PIV and ELDV wind tunnel investigations of the laminar separation bubble above a helicopter blade tip”, Meas. Sci. Technol. 17, 1652–1658, 2006
8. Geissler, W. “Verfahren in der instationären Aerodynamik (Methods in Unsteady Aerodynamics)” DLR-FB 92-03, 1992
9. Geissler, W., Haselmeyer, H., “Investigation of dynamic stall onset” to be published in Aerospace Science and Technology
10. Beam, R., Warming, R.F., “An Implicit Factored Scheme for the Compressible Navier-Stokes Equations“, AIAA J., 16, No.4, April 1978.